ARCHIVES of FOUNDRY ENGINEERING

ISSN (1897-3310)
Volume 9
Issue 4/2009

209 – 214

38/4

Published quarterly as the organ of the Foundry Commission of the Polish Academy of Sciences

Application of digital radiography in evaluation of crack propagation rate in cast steel specimens

R. Sikora[a], B. Piekarski[b], K. Świadek[a], R. Chylińska[b]*

[a] Department of Electrical and Computer Engineering, [b] Institute of Materials Science and Engineering
West Pomeranian University of Technology in Szczecin, Piastów 19, 70–310 Szczecin, Poland
* Corresponding author. E-mail address: renata.chylinska@zut.edu.pl

Received 08.07.2009; accepted in revised form 14.07.2009

Abstract

A technology that utilizes penetrating X-rays is one of the oldest non-destructive testing methods. Digital radiography combines modern digital image processing algorithms with traditional X-ray testing method. The following paper describes the present use of digital radiograms in flaw detection, and the use of identification and classification algorithms in detection of cracks that occur under the effect of thermal fatigue process in creep-resistant steel castings operating as structural elements in heat treatment furnaces. The number and length of cracks formed in specimens of Ø37×5 mm dimensions as a result of shock heating and cooling was evaluated. The test alloy was austenitic cast steel of 30Ni-18Cr type, containing 1.75% Nb and 0.93% Ti (wt.%). It has been indicated that the applied methods of non-destructive testing using digital radiography are fully successful in evaluation of the fatigue crack propagation rate in steel castings.

Key words: Non-destructive testing, Ni-Cr cast steel, Failure, Cracks, Thermal fatigue, Microstructure

1. Introduction

Considering the growing application in industry of high-temperature processes, problems of the thermal fatigue of materials and structures operating under variable temperatures are gaining vivid interest.

Thermal fatigue of elastoplastic materials is mainly caused by plastic deformation due to the effect of external loads (active and passive), temperature gradients, and structural anisotropy [1].

The final consequence of the thermal fatigue process is either deformation of the operating element, or its decohesion – usually preceded by cracks appearing in the examined material. (Fig. 1). Cracks are formed after certain number of cycles, depending on the type of material, shape and dimensions of the element, process parameters, and operating environment [1-3].

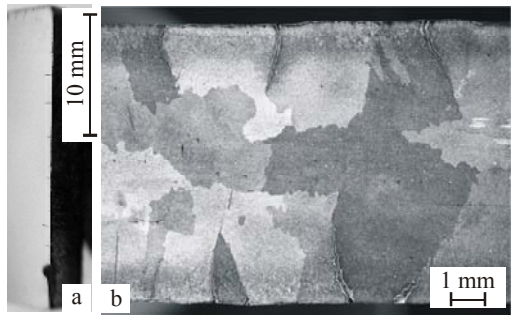

Fig. 1. Thermal fatigue cracks on the specimen edge [4]: a) general appearance, b) image of microstructure indicating the intercrystalline nature of cracks; test material - GX40NiCrSi 36-18

The non-destructive testing methods enable an experimental evaluation of the crack resistance of materials through observations of the time and place of crack nucleation and development, all in function of the thermal fatigue process duration.

A technology that utilizes penetrating X-rays is one of the oldest non-destructive testing methods. For many years, analogue radiography was the only available diagnostic tool. Problems resulting from the application of film technique and progress in technology, due mainly to the development and use of semi-conductors, opened for radiography the door to digitalisation. To improve the quality of the results of examinations, new research techniques have been developed, while the existing ones are improved and enriched with new elements [5].

For many years now, operating within the framework of, among others, the EU FilmFree Project, the Department of Electrical and Computer Engineering at Szczecin University of Technology, Szczecin, has been conducting studies of digital radiography, mainly to test the quality of welds. The Department has a digital radiographic system using light-sensitive image plates (Fig. 2). The image of the examined object is saved on a memory phosphor plate. Then, by means of a special scanner, it is transferred to a computer, and there subjected to digital image processing.

Fig. 2. Test stand equipped with a DR6000 system for digital radiography

Digital radiograms are modified with ImageJ program and image processing algorithms implemented in C++ language (Fig. 3), developed from an analysis of literature and own experience acquired during detection of defects in welds and castings.

This study presents the preliminary results of experiments that have been carried out to better explore the possibilities of practical application of the above described method (see Fig. 3) in detection of cracks formed during the thermal fatigue process in specimens made from the creep-resistant austenitic 30Ni-18Cr steel (Tab. 1), when used for cast structural parts of furnaces for thermal and thermal-chemical treatment [4].

The thermal fatigue resistance of cast steel was evaluated from the number and length of cracks formed in two specimens of Ø37×5 mm dimensions after shock heating and cooling. The specimens were subjected to the three successive cycles of thermal fatigue testing, composed of the following forty operations :

- placing in furnace preheated to 900±5^{o}C,
- holding for 30 minutes,
- cooling in tank with running water.

Cracks were measured after each cycle.

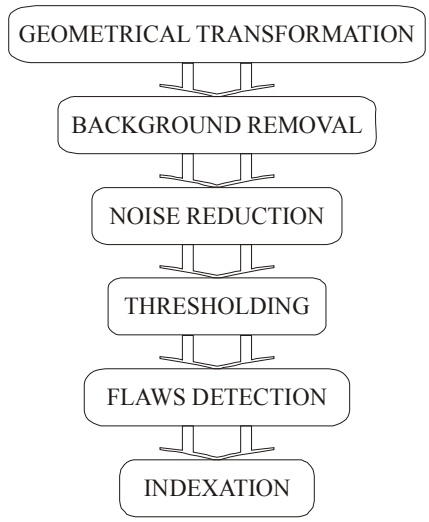

Fig. 3. The successive stages of radiogram processing

Table 1.
Chemical composition of the examined alloy – wt.%

C	Si	Mn	S	P	Cu	Cr	Ni	Nb	Ti
0,29	1,66	0,92	0,012	0,018	0,20	17,5	29,3	1,75	0,93

2. Measurements and results

As a result of the thermal fatigue effect, circumferential cracks running radially towards the specimen centre were formed on the surface of the specimens (Fig. 4a).

The photographs of the specimens were taken with a 120kV X-ray tube and were saved on light-sensitive memory phosphor plates of 10''×12''size. After digitalisation, using a DR6000 scanner, they were written in TIFF format as 16-bit greyscale images.

The determination of ROI was the first step in processing cycle (see Fig. 3), and its aim was to define the region most important for further analysis. Using ImageJ program and the tool called <elliptical mask>, an area outside the specimen was removed as well as an area inside the specimen, the latter one being equal to half-length of the examined object radius (Fig. 4b). Owing to this decision, it was possible to eliminate the effect of cracks that might be formed on the cast specimen surface as a result of marking this surface with numbers used in later identification.

The next step in digital image processing was background removal. Due to this operation, the obtained image comprised only the investigated defects, i.e. cracks, possibly also some

distortions caused by noise during radiographic image capture and digitalisation (Fig. 5a). The image was processed using a rectangular mask of 31×31 pixel size. The mask was dragged over all lines and columns of the image. A median of the increasingly ordered vector of the brightness of all pixels covered by the mask and belonging to the environment of the examined point was ascribed to every point on the resultant image [6-8].

After median filtration of the image, its background free from the flaws and disturbances was generated (Fig. 5b). It was next subtracted from the input image, leaving only cracks and possible distortions.

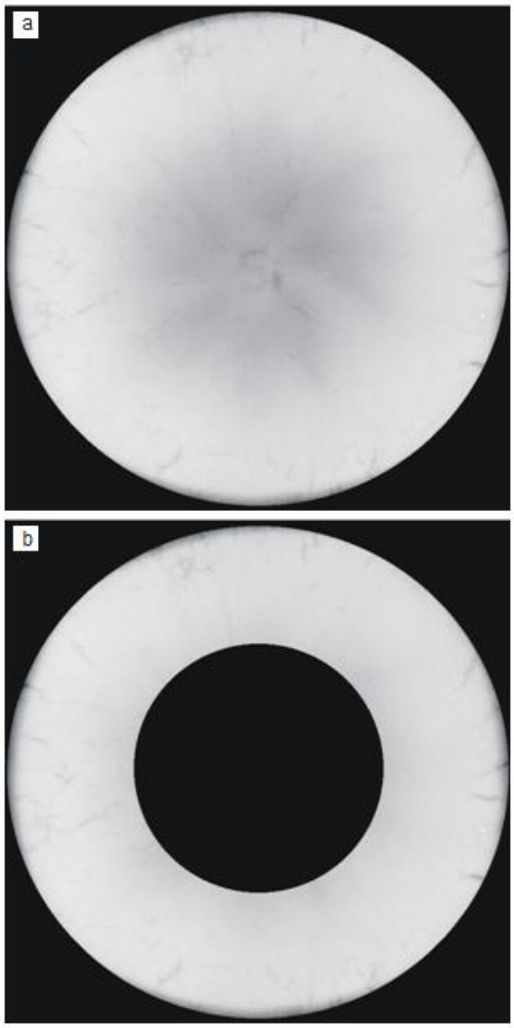

Fig. 4. Original image (a), and the same image after ROI determination (b)

To remove the remaining small disturbances, the <erosion> tool was used (Fig. 6a). Erosion enables morphological transformations, due to which the image is processed with a structuring element, which in this particular case was a rectangular mask of 3×3 pixel size (see equation (1)).

$$I'(m,n) = \min_{m_i,n_i \in A(m,n)} (I(m_i,n_i) \quad (1)$$

where:
I'(m,n) – the value of respective point in the resultant image,
A(m,n) – the structuring element with central point of coordinates (m,n).

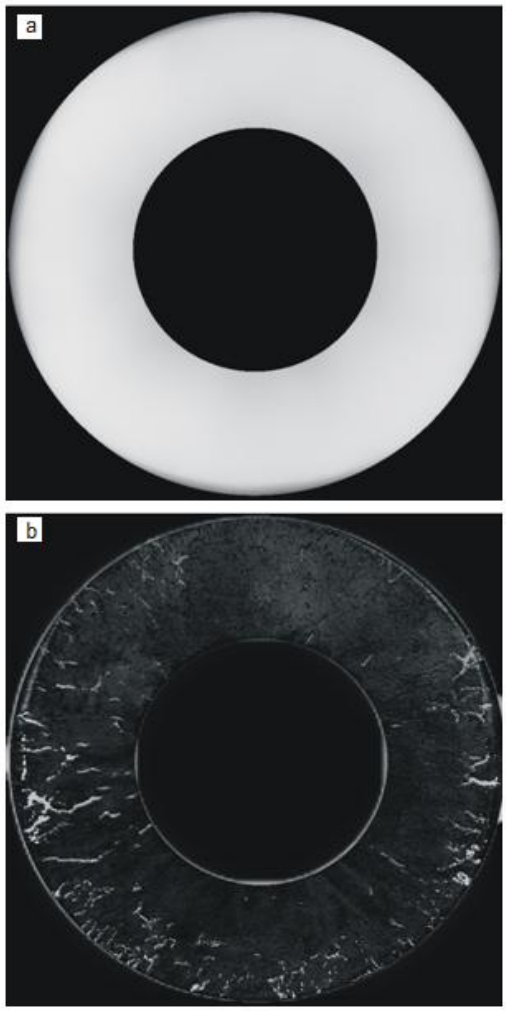

Fig. 5. Background generated with median filter (a), and the appearance of image after background removal (b)

To the central point of the structuring element, a minimum value of the brightness of all the neighbouring points was ascribed, and saved in the resultant image (see equation (1)). Then, the structuring element was drawn over all lines and columns of the image. A drawback of the <erosion> mode of operation was loss of some data (mainly regarding small cracks) and border "cut off" in the case of larger defects [9-11]. So, to reproduce the real (true) image, a transformation reverse to <erosion> was performed (Fig. 6b). In the same way, now a maximum value of the brightness of all pixels of the neighbouring points was ascribed to the examined point (see equation 2).

$$I'(m,n) = \max_{m_i,n_i \in A(m,n)} (I(m_i,n_i)) \quad (2)$$

This transformation is called <dilation>. Combined alternate application of <erosion> and <dilation> is called <opening>.

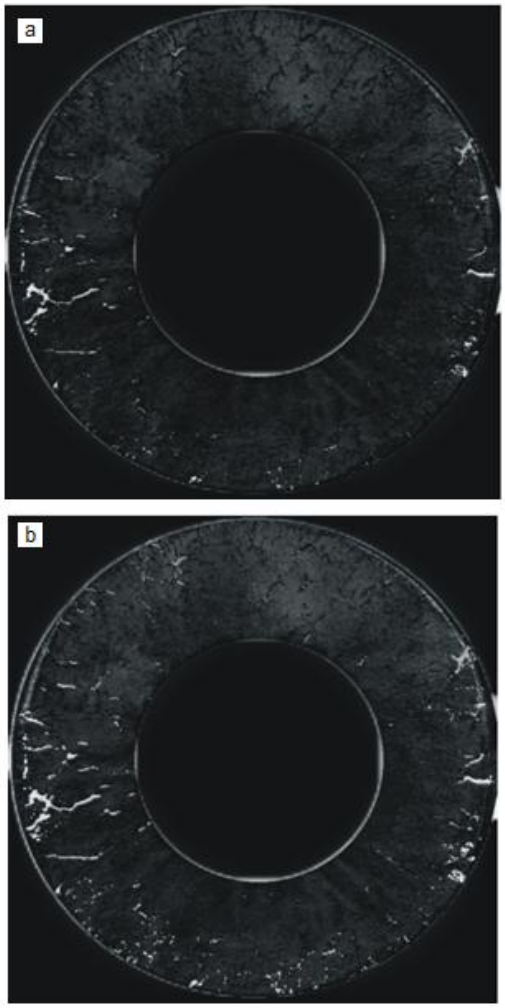

Fig. 6. The image after erosion (a) and opening (b)

The application of <opening> function does not allow us to reproduce small cracks (≤3pix), removed when operating in <erosion> mode, but the percentage of lost information has a negligible effect on the final result of the examinations [14].

Binarisation is the next step in image transformation. Its aim is to reduce considerably the information generally available in processed image. For every image, basing on respective histograms, the values of brightness, otherwise called threshold values, are individually chosen [12]. All pixels with values of the brightness above this threshold are classified as "1", while all other pixels with values below the threshold are classified as "0" (see equation 3) (Fig. 7). In the case under discussion, binarisation with "threshold below" was applied [12, 13].

$$I'(m,n) = \begin{cases} 0; & I(m,n) \leq a \\ 1; & I(m,n) > a \end{cases} \quad (3)$$

where:
I'(m,n) – the value of respective point in the resultant image,
I(m,n) – the brightness of pixel in the examined image,
a – the binarisation threshold.

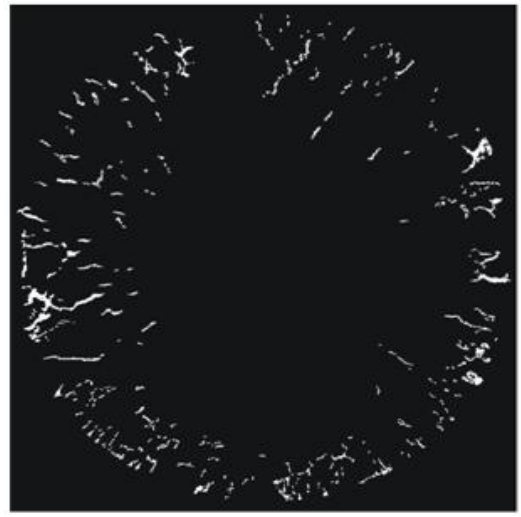

Fig. 7. The image after thresholding

To obtain an image of the defects in the form of lines surrounding the cracks, the operation of <skeletonising> is performed. It consists in replacing objects with a set of curves one pixel wide (Fig. 8a). The said curves are composed of a set of points that are parallel to at least two points located in the edge of the examined object. The algorithm operating this function is similar to <erosion> and <dilation>, the only difference is that now the applied structuring element has the following form of equation (4):

$$\begin{bmatrix} 0 & X & X \\ 0 & 1 & 0 \\ 0 & 0 & 0 \end{bmatrix}, \text{ where } X \text{ – the examined pixel} \quad (4)$$

The use of a structuring element of this type prevents the formation of additional „artefacts", i.e. extra „branching" of the crack skeleton, characterised by a shape substantially different from the shape of a line assumed to run from the specimen edge to its centre [14].

To determine the length of individual cracks, their number, and total length of all cracks, the determination of each detected crack is necessary. This task is accomplished by the function of <indexation>. The said operation consists in ascribing to each object (crack) one of the brightness levels (from 0 to 65535), and in ascribing next this value to every pixel that belongs to the examined object (Fig. 8b). Since the operation of <skeletonising> has already been performed at an earlier stage of the procedure, the length of the cracks is now equal to their surface area, and so to the number of pixels in resultant image with the ascribed index (crack number).

Due to the last performed operation, the number and length of cracks formed in the successive fatigue cycles was determined. The obtained results of the measurements are compared in Table 2 and Fig. 9.

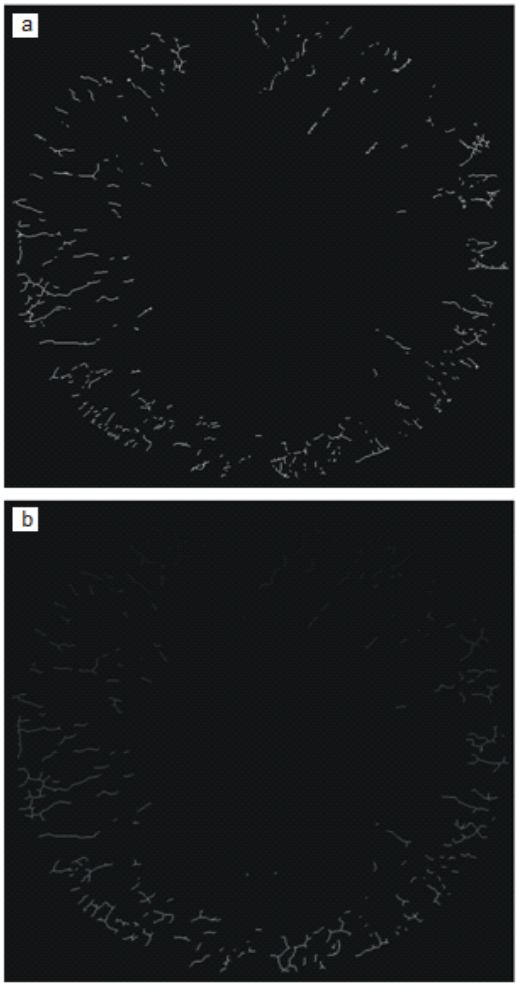

Fig. 8. The image after skeletonising (a) and indexation (b)

Table 2.
The number of detected cracks (Nc) and their total length (ΣD); the results of measurements obtained for specimen 1 / specimen 2

No cycle	Nc	ΣD, [pix]
1	42 / 39	830 / 889
2	86 / 76	1774 / 2112
3	130 / 144	3808 / 4560

3. Summary

The obtained results of the measurements and computations have proved that the method of non-destructive testing using digital radiography, developed by the Department of Electrical and Computer Engineering, Szczecin University of Technology, Szczecin, can be used with full success in evaluation of the propagation rate of fatigue cracks in metallic materials.

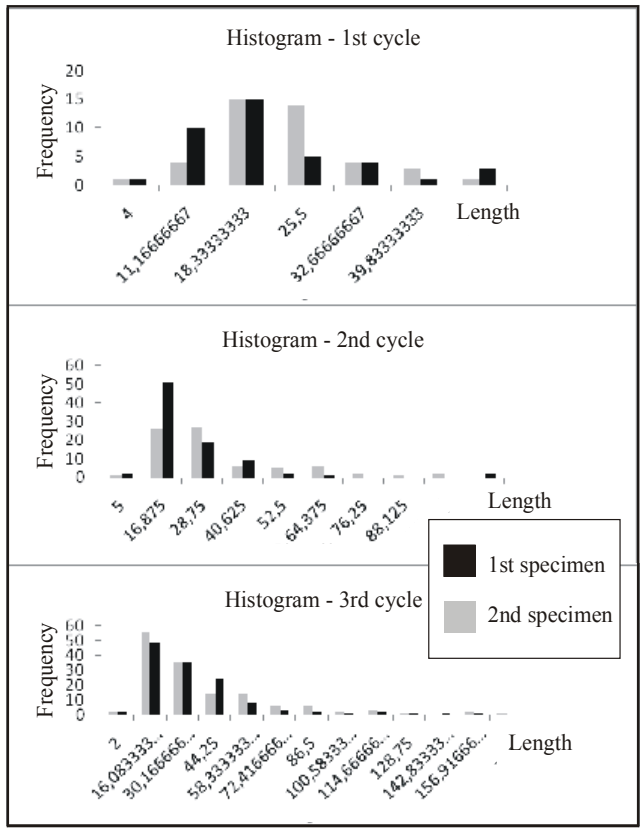

Fig. 9. The distribution of crack length values in specimens after the successive thermal fatigue cycles

The presented results of the investigations enable formulation of the following general conclusions:

1. The applied research method is an effective tool in both qualitative and quantitative description of the crack resistance of materials, basing on the number and length of cracks determined after each cycle of the shock heating and cooling.
2. More complete description of the investigated process of degradation requires more complete set of tools, especially of those that enable, from the technical point of view, measurement of the crack depth; the longest cracks determine the active cross-section of an operating element.

The formerly conducted investigations as well as the present studies can serve as a basis for the following conclusions (this time of a more utilitarian nature) regarding the thermal fatigue damage of materials:

1. While running from the specimen surface to its centre, the cracks follow a broken line course; most probably they are running along the grain boundaries (Figs. 6-8).
2. The relationship between the number of fatigue cycles and the number and total length of cracks is of an approximately linear character (Table 2).

3. After each thermal fatigue cycle, the fraction of short cracks increases in the total number of cracks (Fig. 9).
4. Examining the images of the specimens after the last test cycle (Fig. 8) it is interesting to note that also secondary cracks of orientation normal to the axial cracks have been formed. They indicate the possibility of the specimen edges being crushed if the test continues for a longer time.
5. The susceptibility of the austenitic 30Ni-18Cr cast steel with additions of niobium and/or titanium to crack formation can be interrelated with changes in its phase composition [15].

References

[1] R. Żuchowski, Analiza procesu zniszczenia podczas zmęczenia cieplnego metali. Prac. Nauk. Polit. Wrocławskiej, Wrocław 1986. Monografie nr 18.

[2] A. Weroński, T. Hejwowski, Problematyka trwałości elementów pracujących przy podwyższonych temperaturach. Wydaw. Polit. Lubelskiej, Lublin 1993.

[3] A. Hernas, Żarowytrzymałość stali i stopów – cz. I. Wydaw. Polit. Śląskiej, Gliwice 1999.

[4] B. Piekarski, Odlewy ze staliwa austenitycznego pracujące w piecach do nawęglania – teoretyczne i praktyczne aspekty podwyższania trwałości. Prac. Nauk. PS nr 573, Szczecin 2003.

[5] R. Sikora, T. Chady, W. Ruciński, K. Świadek, Radiografia cyfrowa, Przegląd Elektrotechniczny, 12/2008, pp. 274-277.

[6] Z.G. Zhou, S. Zhao, and Z.G. An, Research On Automatic Inspection Technique Of Real-Time Radiography For Turbine-Blade, Proceedings of World Conference on NDT, 2004 – Montreal, Canada.

[7] N. Nacereddine, M. Tridi, L. Hamami, D. Zjou, Statistical Tools for Weld Defect Evaluation in Radiographic Testing, Proceedings of European NDT Conference, 2006 – Berlin, Germany.

[8] D. Mery, T. Jaeger, D. Filbert, A review of methods for automated recognition of castings defect, Insight Vol 44, No7, July 2002.

[9] A. G. Vincent, V. Rebuffel, R. Guillemaud, L. Gerfault, P. Y. Coulon, Defect detection in industrial casting components using digital X-ray radiography, Insight Non Destructive Testing and Condition Monitoring, October 2002, Vol. 44, pp 623-627.

[10] Gueudre C., Moysan J., Corneloup G., Automatic image processing in radioscopic testing, Review of Progress in Quantitative Nondestructive Evaluation: Volume 20. AIP Conference Proceedings, Volume 557, pp. 740-747 (2001).

[11] D. Mery, Th. Jaeger, D. Filbert, A review of methods for automated recognition of casting defects, Insight, vol. 44, n. 7, pp. 428–436, 2002.

[12] T. Chady, M. Caryk, Selected Algorithms of Background Generation Used for Flaw Detection in Welded Joints, Review Of Progress In Quantitative Nondestructive Evaluation: 34th Annual Review of Progress in Quantitative Nondestructive Evaluation. AIP Conference Proceedings, Volume 975, pp. 453-460 (2008).

[13] R. Sikora, P. Baniukiewicz, T. Chady, W. Ruciński, K. Świadek, M. Caryk, P. Lopato, Comparison of Selected Weld Defect Extraction Methods, Review Of Progress In Quantitative Nondestructive Evaluation: 34th Annual Review of Progress in Quantitative Nondestructive Evaluation. AIP Conference Proceedings, Volume 975, pp. 1034-1041 (2008).

[14] R. Tadeusiewicz, P. Korohoda, Komputerowa analiza i przetwarzanie obrazów, Wydawnictwo Fundacji Postępu Telekomunikacji, Kraków 1997.

[15] M. Garbiak, K. Świadek, B. Piekarski, Phase composition and thermal fatigue resistance of Ni-Cr cast steel. Mater. 17th IFHTSE Congress 2008, Oct. 27-30 2008, Kobe, Japan, P50, p. 266.